Sandeep Pokharia*, Rachana Joshi, Mamta Pokharia, Swatantra Kumar Yadav and Hirdyesh Mishra

A density functional theory insight into the structure and reactivity of diphenyltin(IV) derivative of glycylphenylalanine

DOI 10.1515/mgmc-2016-0009
Received March 8, 2016; accepted July 20, 2016; previously published online August 12, 2016

Abstract: The quantum-chemical calculations based on density functional theory (DFT) have been performed on the diphenyltin(IV) derivative of glycyl-phenylalanine (H_2L) at the B3LYP/6-31G(d,p)/LANL2DZ(Sn) level of theory without any symmetry constraint. The harmonic vibrational frequencies were computed at the same level of theory to find the true potential energy surface minima. The various geometrical and thermochemical parameters for the studied complex are obtained in the gas phase. The atomic charges at all the atoms were calculated using the Mulliken population analysis, the Hirshfeld population analysis, and the natural population analysis. The charge distribution within the studied complex is explained on the basis of molecular electrostatic potential maps, frontier molecular orbital analysis, and conceptual DFT-based reactivity (global and local) descriptors, using the finite difference approximation method. The nature of O-Sn, N-Sn, N→Sn, and C-Sn bonds is discussed in terms of the conceptual DFT-based reactivity descriptors. The structural analysis of the studied complex has been conducted in terms of the selected bond lengths and bond angles. The structural and the atomic charge analyses suggest a distorted trigonal bipyramidal arrangement consisting of negatively charged centers around the positively charged central Sn atom.

Keywords: conceptual DFT; diphenyltin(IV); glycylphenylalanine; organotin(IV); reactivity descriptors.

***Corresponding author: Sandeep Pokharia,** Organometallics and Molecular Modelling Group, Chemistry Section, M.M.V., Banaras Hindu University, Varanasi 221005, India,
e-mail: sandeepp@bhu.ac.in
Rachana Joshi and Mamta Pokharia: Organometallics and Molecular Modelling Group, Chemistry Section, M.M.V., Banaras Hindu University, Varanasi 221005, India
Swatantra Kumar Yadav and Hirdyesh Mishra: Physics Section, M.M.V., Banaras Hindu University, Varanasi 221005, India

Introduction

In recent decades, the chemistry of organotin(IV) compounds has drawn considerable research interest because of their structural diversity and wide range of synthetic and biological applications (Nath, 2008). These compounds, which are characterized by the presence of tetravalent Sn centers and at least one covalent Sn-C bond, often exhibit previously tetravalent Sn atoms expanding their coordination number and becoming hypervalent on inter- and/or intramolecular interactions with electron donor atoms. The appearance of such additional interactions results from the large size of Sn atom, the availability of low-lying empty 5d atomic orbitals, and the pronounced electron-acceptor ability of the Sn atoms (Pellerito and Nagy, 2002). However, apart from such unique structural features, organotin(IV) compounds hold significance owing to their possible use as potential biologically active nonplatinum chemotherapeutic metallopharmaceuticals having antitumor activity (Alama et al., 2009; Arjmand et al., 2014; Carraher and Roner, 2014). The speciation of organotin(IV) compounds in the biological systems has revealed that their antiproliferative activity depends on the availability of coordination positions at Sn center, number of Sn-C bonds, electronic and geometrical properties, mode of coordinating ligands, occurrence of relatively stable ligand-Sn bonds (e.g. Sn-N and Sn-S), and their slow hydrolytic decomposition (Pellerito and Nagy, 2002). As a result, in the last decades, several organotin(IV) derivatives of dipeptides have been modeled for metal-protein interactions and have also been shown to exhibit a wide range of biological activities (Katsoulakou et al., 2008; Nath et al., 2009; Girasolo et al., 2010). These studies have provided an impetus to understand the electronic properties of such derivatives so as to formulate a theoretical basis for the experimental observations.

In the contemporary research, the quantum-chemical methods based on density functional theory (DFT) have been used for understanding the electronic structure of molecules to correlate the calculated structural features

with the experimental observations. The DFT-based methods have reasonably accounted for the electron correlation for organotin(IV) derivatives with heterodonor ligands; hence, several studies have successfully calculated the geometric structures for such systems by quantum-chemical calculations performed within a domain of DFT (Girichev et al., 2012; Latrous et al., 2013; Thomas et al., 2013; Matczak, 2015). Further, the study of conceptual DFT-based descriptors is indispensable to comprehend the electronic structure of an organotin(IV) complex, which has far-reaching consequences on its structure and reactivity. Moreover, with an aim to design new molecular entities possessing unique structural features and broad range of synthetic and biological applications, we have systematically initiated efforts on the theoretical investigation of the organotin(IV)-peptide system. Such studies hold significance as they will provide insight into the nature of interaction of peptide molecule with organotin(IV) moiety, and the reactivity behavior of the organotin(IV)-peptide complex will thus be formed. As a part of our systematic study on the structure and reactivity of organotin(IV)-peptide system in light of conceptual DFT-based quantum-chemical calculations (Pokharia, 2015), the present work highlights the theoretical investigation on previously synthesized diphenyltin(IV) derivative of glycylphenylalanine (Ph_2SnL, where L is the dianion of glycylphenylalanine) (Figure 1A; Nath et al., 2004), so as to obtain a theoretical description for the nature of interaction of heterodonor atoms (ONN) in the dipeptide molecule with diphenyltin(IV) moiety within the complex and also its reactivity behavior. The structure and the nature of interaction of the studied complex are investigated in terms of the calculated atomic charges and frontier molecular orbital (FMO) analysis, and its reactivity is interpreted in light of conceptual DFT-based global and local reactivity descriptors.

Results and discussion

Geometry optimization and structural analysis

The ground-state optimized geometry in the gas phase of Ph_2SnL calculated at the B3LYP/6-31G(d,p)/LANL2DZ(Sn) computational level of theory is presented in Figure 1B (cf. Figure 1A for atom number notation). The frequency analysis indicates that the optimized geometric configuration is the local minima on the potential energy surface (PES) of Ph_2SnL. The selected bond lengths and bond angles in Ph_2SnL are presented in Table S1 (Supplementary Material).

As presented in Figure 1B, the calculated geometric environment around the central Sn atom in Ph_2SnL is considerably distorted with terminal carboxylate oxygen O17 (Sn-O17=2.019 Å) and terminal amino nitrogen N1 (Sn-N1=2.430 Å) in the axial positions, and deprotonated peptide nitrogen N9 (Sn-N9=2.058 Å) and two phenyl carbons C30 and C41 (Sn-C30=2.126 Å and Sn-C41=2.124 Å) in the equatorial plane. The calculated equatorial angle C30-Sn-C41 in Ph_2SnL is 118.6°, which is close to that in experimentally reported penta-coordinated diorganotin(IV) dipeptides [e.g. Ph_2Sn(Gly-Gly), 117.5° (Huber et al., 1977); *n*-Bu_2Sn(Gly-Val), 125.3° (Mundus-Glowacki et al., 1992)] but smaller to that experimentally reported in *n*-Bu_2Sn(Trp-Gly), 151.6° (Nath et al., 2009), and Me_2Sn(Tyr-Phe)·MeOH, 136.4° (Nath et al., 2008). The distortion in the molecule is evident from the calculated axial angle N1-Sn-O17 of 153.4°, which is close to the experimentally reported values for *n*-Bu_2Sn(Trp-Gly), 147.9° (Nath et al., 2009), and Me_2Sn(Tyr-Phe)·MeOH, 149.6° (Nath et al., 2008). Further, various bond angles involving the central Sn atom suggest a distorted trigonal bipyramidal arrangement. Also, there seems to be a change in

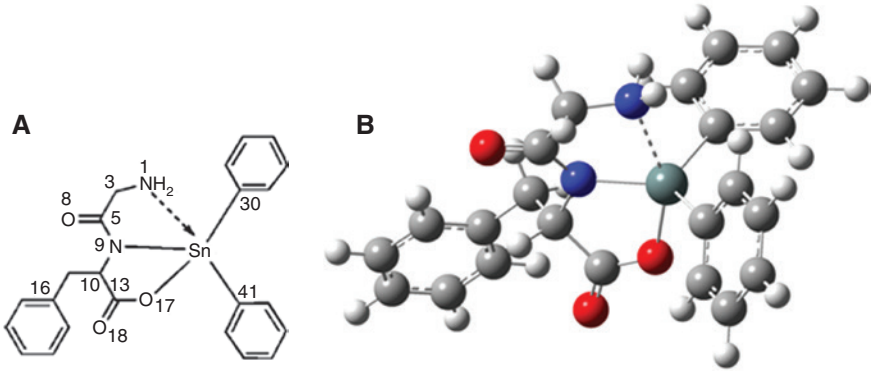

Figure 1: Molecular geometry of diphenyltin(IV) derivative of glycylphenylalanine.
(A) Structure (along with the atom number) of the diphenyltin(IV) derivative of glycylphenylalanine (Ph_2SnL). (B) Ground-state optimized geometry (in gas phase) of Ph_2SnL calculated at the B3LYP/6-31G(d,p)/LANL2DZ(Sn) level of theory.

bond length of various bonds involving N1, N9, and O17 in Ph_2SnL relative to H_2L, indicating the electron redistribution around the central Sn atom through these coordinating atoms. The calculated distorted trigonal bipyramidal arrangement is consistent with previously reported geometry of diorganotin(IV) derivatives of dipeptides (Huber et al., 1977; Mundus-Glowacki et al., 1992; Katsoulakou et al., 2008; Nath et al., 2008, 2009; Girasolo et al., 2010).

The various energetic and thermochemical parameters for Ph_2SnL in the gas phase have been calculated at 1 atm and 298.15 K at the B3LYP/6-31G(d,p)/LANL2DZ(Sn) level of theory, and the results are presented in Table S2. The total energy of Ph_2SnL calculated after zero-point correction and the thermal correction to energy, enthalpy, and Gibbs free energy have been estimated; for instance, its calculated total energy after thermal correction to Gibbs free energy, which is the sum of electronic and thermal free energies (G=H-TS) (Foresman and Frisch, 1996), is -1227.9881 a.u. The contribution to internal thermal energy (E_{tot}), entropy (S_{tot}), and constant volume molar heat capacity (CV_{tot}) has the value for Ph_2SnL as 271.22 kcal/mol, 189.48 cal/mol-K, and 101.48 cal/mol-K, respectively.

Atomic charges and molecular electrostatic potential (MEP) map

The MEP is created in the space around a molecule by its nuclei and electrons and is related to the electron density. It holds significance because it provides substantial insight into the sites within the molecule where the electron distribution effect is dominant, for example, for the intermolecular association and molecular properties of small molecules, predicting molecular reactive behavior, and analyzing processes based on the 'recognition' of one molecule by another, such as between a drug and its cellular receptor, because it is through their potentials that the two species first 'see' each other (Politzer et al., 1985). The MEP surface of Ph_2SnL calculated on the ground-state optimized geometry in gas phase at the B3LYP/6-31G(d,p)/LANL2DZ(Sn) level of theory is presented in Figure 2A. The different values of the electrostatic potential at the surface are represented by different colors and potential increases in the order red<orange<yellow <green<blue. As evident from the MEP map (Figure 2A), the greater regions of the complex are of intermediary potential (green coded regions), but because the green color is toward the increasing range of the potential (toward the blue color), the complex possesses smaller electronegativity with electron-deficient regions having preference for an approach by nucleophiles.

The calculation of effective atomic charges is significant whenever quantum-chemical calculations are applied to molecular systems because they affect dipole moment, molecular polarizability, and electronic structure. In such systems, the atomic charges are attributed through population analysis. To study electrostatic arguments that would explain the probable structure and reactivity of Ph_2SnL, an electron density distribution analysis has been performed on the basis of atomic charges determined by the Mulliken population analysis (MPA), the Hirshfeld population analysis (HPA), and the natural population analysis (NPA) charge schemes in the gas phase within Ph_2SnL, at the B3LYP/6-31G(d,p)/LANL2DZ(Sn) level of theory, and the results based on these schemes for

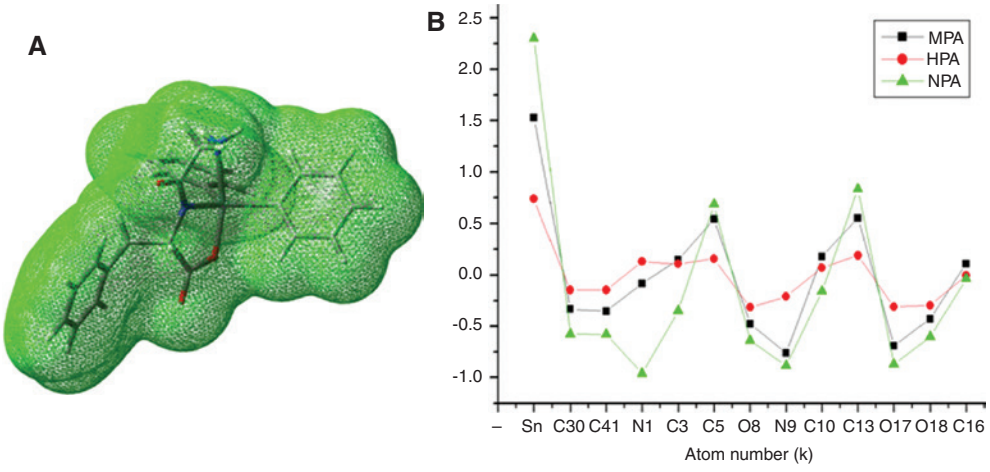

Figure 2: Molecular electrostatic potential (MEP) map and atomic charges for diphenyltin(IV) derivative of glycylphenylalanine. (A) Molecular electrostatic potential (MEP) map. (B) Plot of atomic charges at the selected atoms based on MPA, HPA, and NPA for the ground-state optimized geometry (in the gas phase) for Ph_2SnL calculated at the B3LYP/6-31G(d,p)/LANL2DZ(Sn) level of theory.

the selected atoms in Ph_2SnL are presented in Figure 2B and Table S3.

The population of the atomic orbitals suggest that in Ph_2SnL, the natural electron configuration of the central Sn atom is [core]$5s^{0.78}5p^{0.92}6p^{0.01}$, which differs significantly from $Ph_2Sn(IV)^{2+}$ cation configuration [core]$5s^2$. The absolute value of the natural charge of the central Sn atom in Ph_2SnL on the basis of NPA is 2.299. Further, the natural electron configuration of coordinating oxygen atom (O17) is [core]$2s^{1.70}2p^{5.16}3d^{0.01}$, amino nitrogen (N1) is [core]$2s^{1.43}2p^{4.52}3p^{0.01}$, and deprotonated peptide nitrogen (N9) is [core]$2s^{1.35}2p^{4.52}3p^{0.01}$. The absolute values of the natural charge of N1, N9, and O17 on the basis of NPA are approximately -0.960, -0.884, and -0.872, respectively. Moreover, the natural electron configuration of two carbon atoms (covalently bonded to the central Sn atom), viz., C30 and C41, is [core]$2s^{1.05}2p^{3.50}3p^{0.02}$. The absolute values of the natural charge of C30 and C41 on the basis of NPA are approximately -0.576 and -0.578, respectively. The existence of the high positive value of charge at the central Sn atom and such oppositely charged centers around it further confirms the ionic interaction in the Sn-O and Sn-N bonds, resulting in the formation of coordinate/dative bonds between the ONN system of deprotonated H_2L and $Ph_2Sn(IV)$ moiety. The results, as presented in Figure 2B, indicate that the most negative atomic charges are attributed to oxygen, nitrogen, and organotin(IV) carbon atoms in the Ph_2SnL derivative. Similarly, results are reported for tin systems with ligands having heterodonor atoms (Girichev et al., 2012; Latrous et al., 2013; Matczak, 2015). The population analysis based on MPA, HPA, and NPA also indicates an ionic interaction in these bonds (Table S3). The presence of such an ionic interaction in Ph_2SnL is significant as it may lead to a slow hydrolytic decomposition of Sn-O/N bonds, suggesting that the complex can exhibit potential activity, such as antiproliferative activity owing to the existence of $R_2Sn(IV)^{2+}$ (R=Ph) moiety in the biological medium.

Conceptual DFT-based global reactivity descriptors

The molecular properties and the conceptual DFT-based global reactivity descriptors for the ground-state optimized geometries in the gas phase of H_2L and Ph_2SnL, calculated using finite difference approximation, are presented in Table 1. The results indicate that the dipole moment that accounts for the existence of charged separated regions within the system is greater for Ph_2SnL (10.35 Debye) in comparison with H_2L (3.31 Debye). The ionization potential (IP) and the electron affinity (EA) for Ph_2SnL are lower than that for H_2L. As a result, the band gap (ΔE) for Ph_2SnL (7.89 eV) is lower than H_2L (9.50 eV).

Table 1: Calculated molecular properties and conceptual DFT-based global reactivity descriptors for the ground-state optimized geometries (in gas phase) of Gly-Phe (H_2L) at B3LYP/6-31G(d,p) and Ph_2SnL at the B3LYP/6-31G(d,p)/LANL2DZ(Sn) level of theory.

Parameter/property	System	
	Gly-Phe (H_2L)	Ph_2SnL
E_N (a.u.)[a]	-762.824913	-1228.331213
E_{N+1} (a.u.)	-762.773851	-1228.313607
E_{N-1} (a.u.)	-762.526946	-1228.059070
Dipole moment (Debye)[b]	3.31	10.35
IP (eV)[c]	8.11	7.41
EA (eV)[d]	-1.39	-0.48
ΔE (eV)[e]	9.50	7.89
E_{HOMO} (eV)[f]	-8.11	-7.41
E_{LUMO} (eV)[g]	1.39	0.48
Electronic chemical potential (μ) (eV)[h]	-3.36	-3.46
Electronegativity (χ) (eV)[i]	3.36	3.46
Global hardness (η) (eV)[j]	9.50	7.89
Global softness (S) (/eV)[k]	0.11	0.13
Electrophilicity index (ω) (eV)[l]	0.59	0.76

[a]E_N, E_{N+1}, and E_{N-1} are the total energies of the system containing, respectively, N, N+1, and N-1 electrons.
[b]Dipole moment for the system containing N number of electrons.
[c]IP is the ionization potential given by E_{N-1}-E_N.
[d]EA is the electron affinity given by E_N-E_{N+1}.
[e]ΔE is the band gap given by IP-EA.
[f]Energy of the highest occupied molecular orbital as -E_{HOMO}=IP.
[g]Energy of the lowest unoccupied molecular orbital as -E_{LUMO}=EA.
[h]Electronic chemical potential of the system given by $\left(\frac{E_{HOMO}+E_{LUMO}}{2}\right)$ (Geerlings et al., 2003).
[i]Electronegativity of the system given by -μ.
[j]Global hardness of the system given by E_{LUMO}-E_{HOMO} (Parr and Pearson, 1983; Geerlings et al., 2003).
[k]Global softness of the system given by 1/η (Yang and Parr, 1985; Geerlings et al., 2003).
[l]Electrophilicity index of the system given by $\mu^2/2\eta$ (Parr et al., 1999; Geerlings et al., 2003; Chattaraj et al., 2006).

The FMO analysis is significant from the perspective of understanding the distribution of charge density within a system as it helps in estimating the energies and the type of frontier molecular orbitals because these orbitals are the sites of exchange of charge density, which leads to the interaction between molecules. The FMO analysis for Ph_2SnL has been performed through the Koopman's approximation within the molecular orbital theory (Geerlings et al., 2003), and the E_{HOMO} and the E_{LUMO} energies are

presented in Table 1. The E_{HOMO} and the E_{LUMO} plots along with the band gap (ΔE) in the gas phase, as presented in Figure 3, indicate that, in Ph_2SnL, the highest occupied molecular orbital (HOMO) is concentrated over the dipeptide, whereas the lowest unoccupied molecular orbital (LUMO) is concentrated around the central Sn atom and organic residues in organotin(IV) moiety, indicative of the interaction of H_2L with Ph_2Sn(IV) moiety through deprotonated oxygen (O17) and peptide nitrogen (N9) atoms, as reported previously for other diorganotin(IV)-dipeptide systems (Huber et al., 1977; Mundus-Glowacki et al., 1992; Nath et al., 2008, 2009; Girasolo et al., 2010). Further, the FMO analysis suggests that upon interaction with an electron donor/acceptor, in Ph_2SnL, the region around the central Sn atom will behave as an acceptor of charge density, whereas the dipeptide region (L^{2-}) will behave as a donor of charge density. Moreover, the studied complex interacts with macromolecular receptors through the central Sn atom upon the slow hydrolysis (owing to ionic interaction) of Sn-O/N bonds.

The global reactivity descriptors calculated based on FMO analysis are tabulated in Table 1. The electronic

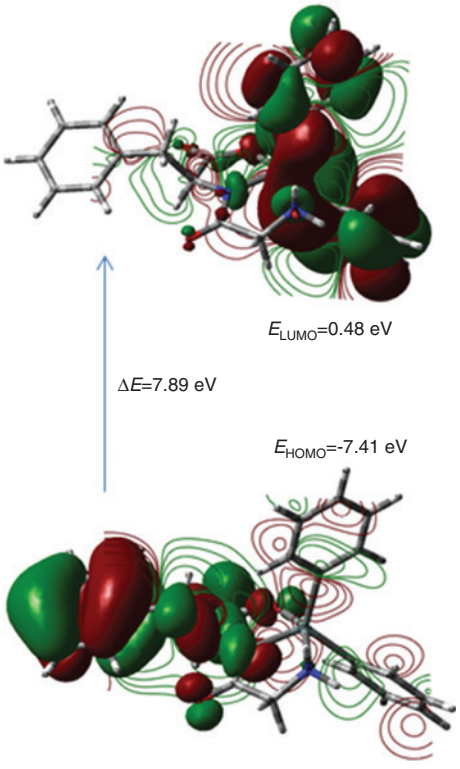

Figure 3: Highest occupied molecular orbital (HOMO) and lowest unoccupied molecular orbital (LUMO) plots along with band gap (ΔE) in the gas phase for Ph_2SnL calculated at the B3LYP/6-31G(d,p)/LANL2DZ(Sn) level of theory.

chemical potential (μ), which measures the sensitiveness of the system's energy to a change in the number of electrons at fixed external potential $\left[\mu=\left(\frac{\partial E}{\partial N}\right)_{v(\vec{r})}\right]$ (Geerlings et al., 2003), is greater for Ph_2SnL in comparison with H_2L, indicating that the energy of the complex is more sensitive toward the change in the number of electrons. Further, because electronegativity (χ) is negative of μ, it increases on complex formation. The global hardness (η), which is the resistance of the electronic chemical potential to changes in the number of electrons $\left[\eta=\left(\frac{\partial^2 E}{\partial N^2}\right)_{v(\vec{r})}=\left(\frac{\partial \mu}{\partial N}\right)_{v(\vec{r})}\right]$ (Parr and Pearson, 1983), can be regarded as a resistance to charge transfer, whereas global softness (S), which is the inverse of the global hardness $\left[S=\frac{1}{\eta}=\left(\frac{\partial N}{\partial \mu}\right)_{v(\vec{r})}\right]$ (Yang and Parr, 1985), is a measure of the ease of charge transfer and is associated with high polarizability. The value of η for H_2L is greater than Ph_2SnL, whereas that of S is smaller than Ph_2SnL. Because finite difference approximation to global hardness equates it to band gap, these results indicate that Ph_2SnL with small band gap is more soft and polarizable in comparison with H_2L. Moreover, the electrophilicity index $\left[\omega=-\Delta E\equiv\frac{\mu^2}{2\eta}\right]$, which measures the electrophilic power of a system (Chattaraj et al., 2006) and which can be described as the maximum ability of a molecule to accept electrons in the neighborhood of an electron reservoir (Parr et al., 1999), has a value of 0.76 eV for Ph_2SnL. Because ω is positive for Ph_2SnL and also higher than H_2L, the complex possesses electrophilic power, and assuming the system as electron donor/acceptor, the process will be an energetically favorable process during partial charge transfer. The calculated global reactivity descriptors further suggest that Ph_2SnL can exhibit potential biological activity on its probable interaction with macromolecular receptors because it is soft and polarizable, and charge transfer during such an interaction will be an energetically favorable process.

Conceptual DFT-based local reactivity descriptors

The conceptual DFT-based local reactivity descriptors, such as Fukui function index [$f^{\pm}(k)$] (Parr and Yang, 1984; Geerlings et al., 2003; Roy and Saha, 2010), local softness [$s^{\pm}(k)$] (Geerlings et al., 2003; Roy and Saha, 2010), local electrophilicity [$\omega^{\pm}(k)$] (Geerlings et al., 2003; Chattaraj

et al., 2006; Roy and Saha, 2010), and hardness potential [$\Delta^{\pm}h(k)$] (Geerlings et al., 2003; Saha et al., 2013), considered to predict the regioselectivity of the atoms in Ph_2SnL, have been calculated at all the atoms with three different population analysis schemes, viz., MPA, HPA, and NPA, and the results based on the NPA, HPA, and MPA schemes at the selected atoms of Ph_2SnL are presented in Tables S4, S5, and S6, respectively. The variation of $f^+(k)$ and $s^+(k)$, $f^-(k)$ and $s^-(k)$, $\omega^+(k)$ and $\omega^-(k)$, and $\Delta^+h(k)$ and $\Delta^-h(k)$ at the selected atoms of Ph_2SnL calculated on the basis of MPA, HPA, and NPA charge schemes is presented in Figure 4A–D, respectively.

Because there are some differences between the atomic charges obtained from MPA and NPA schemes (Reed et al., 1985), Fukui indices will be highly dependent on the population analysis method, and the results should therefore be analyzed with greater restraint. The Fukui function $f^+(\vec{r})$ easures the reactivity toward the nucleophilic attack on the system, and its large value at a particular site indicates that the site is capable of accepting electron density. Similarly, the Fukui function $f^-(\vec{r})$ measures the reactivity toward an electrophilic attack on the system, and its large value at a particular site indicates that the site is an electron-donating site (Geerlings et al., 2003). Further, it had been proposed that a larger value of the Fukui function indicates more reactivity (Parr and Yang, 1984), and hence, for a particular atomic center in the molecule, the greater the value of the condensed Fukui function, the more reactive it will be (Roy and Saha, 2010). Moreover, for a nucleophilic attack due to an addition of an electron to the molecule, a positive value for the Fukui function $f^+(\vec{r})$ at a particular atom emphasizes an

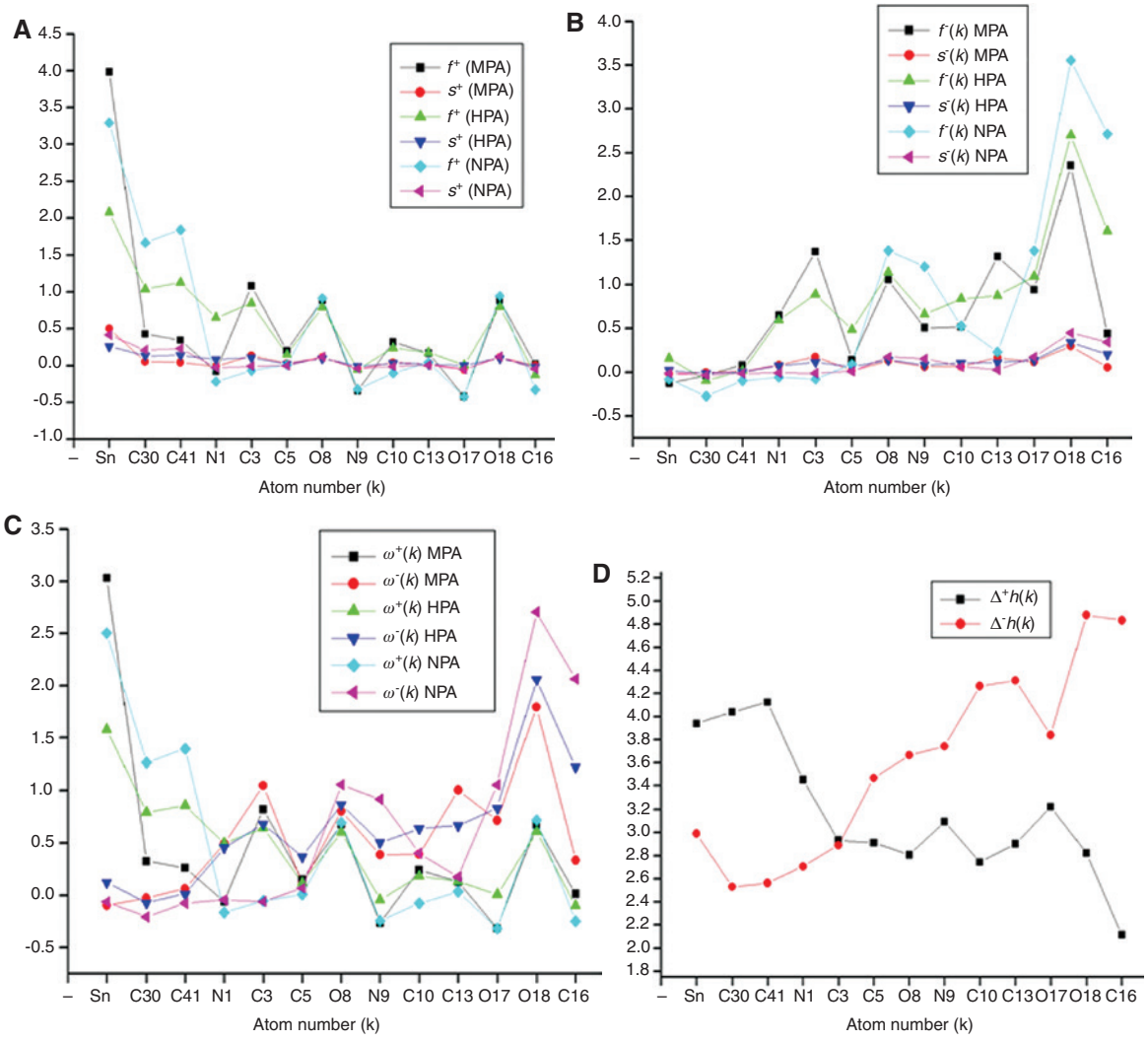

Figure 4: Variation of (A) $f^+(k)$ and $s^+(k)$, (B) $f^-(k)$ and $s^-(k)$, (C) $\omega^+(k)$ and $\omega^-(k)$, and (D) $\Delta^+h(k)$ and $\Delta^-h(k)$ at the selected atoms of Ph_2SnL based on MPA, HPA, and NPA charges, calculated at the B3LYP/6-31G(d,p)/LANL2DZ(Sn) level of theory (all values are given in eV).

increase of atomic population on that position, whereas a negative value means that the electron density is reduced. Similarly, for an electrophilic attack, when an electron is removed from the molecule, a positive value for the Fukui function $f^-(\vec{r})$ at a particular atom emphasizes a decrease of atomic population on that position, whereas a negative value means that the electron density grows larger (Roy and Saha, 2010).

As evident from the results (cf. Figure 4), in Ph_2SnL, the trends based on the values of $f^+(k)$, $s^+(k)$, and $\omega^+(k)$ with all the population scheme suggest that the central Sn atom is an electrophilic site and is more reactive toward a nucleophile and that such an attack increases the atomic population at this center. Similarly, the trends based on the values of $f^-(k)$, $s^-(k)$, and $\omega^-(k)$ with all the population schemes suggest that O18 is the most reactive site toward an electrophilic attack. The results obtained are in accordance with the FMO analysis, which indicates that in Ph_2SnL, the HOMO is concentrated over the dipeptide unit and the LUMO is concentrated around the central Sn atom encompassing the phenyl residues covalently bonded to the central Sn atom. These results outline the general behavior of the central Sn atom in the organotin(IV) complexes in accordance with the previously reported experimental observations, that $R_2Sn(IV)^{2+}$ is an active species in the biological medium (Pellerito and Nagy, 2002). The two variants of the hardness potential, viz., the electrophilic hardness potential $[\Delta^+h(k)]$ and the nucleophilic hardness potential $[\Delta^-h(k)]$, which measures the reactivity toward an approaching nucleophilic and electrophilic reagent, respectively, have also been calculated at all the atoms of Ph_2SnL. The higher the value of $\Delta^+h(k)$ at an atom, the higher the reactivity (i.e. electrophilicity) of that atom toward an approaching nucleophile (Saha et al., 2013). Likewise, the higher the positive value of $\Delta^-h(k)$ for an atom, the higher the reactivity (i.e. nucleophilicity) of that atom toward an approaching electrophile. As evident from the results (cf. Table S4 and Figure 4D), in Ph_2SnL, the trends based on the values of $\Delta^+h(k)$ suggest that C30/C41 (carbon bonded covalently to the Sn atom) is the most reactive site toward an approaching nucleophilic reagent, and the trends based on the values of $\Delta^-h(k)$ suggest that O18 is among the most reactive site toward an approaching electrophilic reagent. Further, in the coordination sphere around the central Sn atom, the higher value of $\Delta^+h(k)$ at the central Sn atom, $N1_{(amino)}$, and C30/C41 indicates that these sites are more reactive toward a nucleophilic reagent. However, the higher value of $\Delta^-h(k)$ at $N9_{(peptidic)}$ and $O17/O18_{(carboxylate)}$ indicates that these sites are more reactive toward an electrophilic reagent.

The variation of relative electrophilicity $\left[\left(\frac{s^+(k)}{s^-(k)}\right)\right]$ and relative nucleophilicity $\left[\left(\frac{s^-(k)}{s^+(k)}\right)\right]$ (Roy et al., 1998; Geerlings et al., 2003) and dual reactivity descriptor $[f^2(k)]$ (Morell et al., 2005) at the selected atoms of Ph_2SnL based on MPA, HPA, and NPA charges is presented in Figure 5A–C, respectively. Because the MPA and the NPA schemes gave negative Fukui index values for some of the atomic sites, a comparative analysis of relative electrophilicity and relative nucleophilicity is presented based on the HPA scheme. The relative electrophilicity helps to locate the preferable site (or atom) in a molecule for a nucleophilic attack on it and it is the electrophilicity of any site as compared with its own nucleophilicity, whereas the relative nucleophilicity helps to locate the preferable site (or atom) in a molecule for an electrophilic attack on it and it is the nucleophilicity of any site as compared with its own electrophilicity (Roy et al., 1998). As evident from the results (cf. Figure 5A and B) based on the HPA scheme, C41 has maximum relative electrophilicity (62.1964), whereas O17 has maximum relative nucleophilicity (135.3333). Further, based on the HPA scheme (cf. Table S5 and Figure 5A), in the coordination sphere around the central Sn atom in Ph_2SnL, the central Sn (13.0191) and the $N1_{(amino)}$ (1.0922) are also potential electrophilic sites and, thus, are the highly preferred sites for a nucleophilic attack, owing to the higher value of relative electrophilicity as compared with relative nucleophilicity. By contrast, C13 (4.9503) and $O18_{(carboxylic)}$ (3.3902) are potential nucleophilic sites (cf. Figure 5B) and, thus, are the highly preferred sites for an electrophilic attack, owing to the higher value of relative nucleophilicity as compared with relative electrophilicity. These results further indicate that in the Ph_2SnL derivative, greater charge density is concentrated over the dipeptide unit. In the dual reactivity descriptor $[f^2(k)]$, a selectivity index is able to characterize both the nucleophilic and the electrophilic behaviors. As evident from the results (cf. Tables S4, S5, and S6), in Ph_2SnL, among the selected atoms, the central Sn atom has the most positive $f^2(k)$ value based on both NPA (3.3729 eV) and HPA (1.9185 eV) schemes (cf. Figure 5C), indicating it to be most susceptible for a nucleophilic attack, whereas $O18_{(carboxylate)}$ has the most negative $f^2(k)$ value based on HPA (-1.9067 eV) and C16 based on NPA (-3.0420 eV) (cf. Figure 5C), indicating these sites to be most susceptible for an electrophilic attack. Furthermore, as evident from the results based on the HPA scheme (cf. Figure 5C), in the

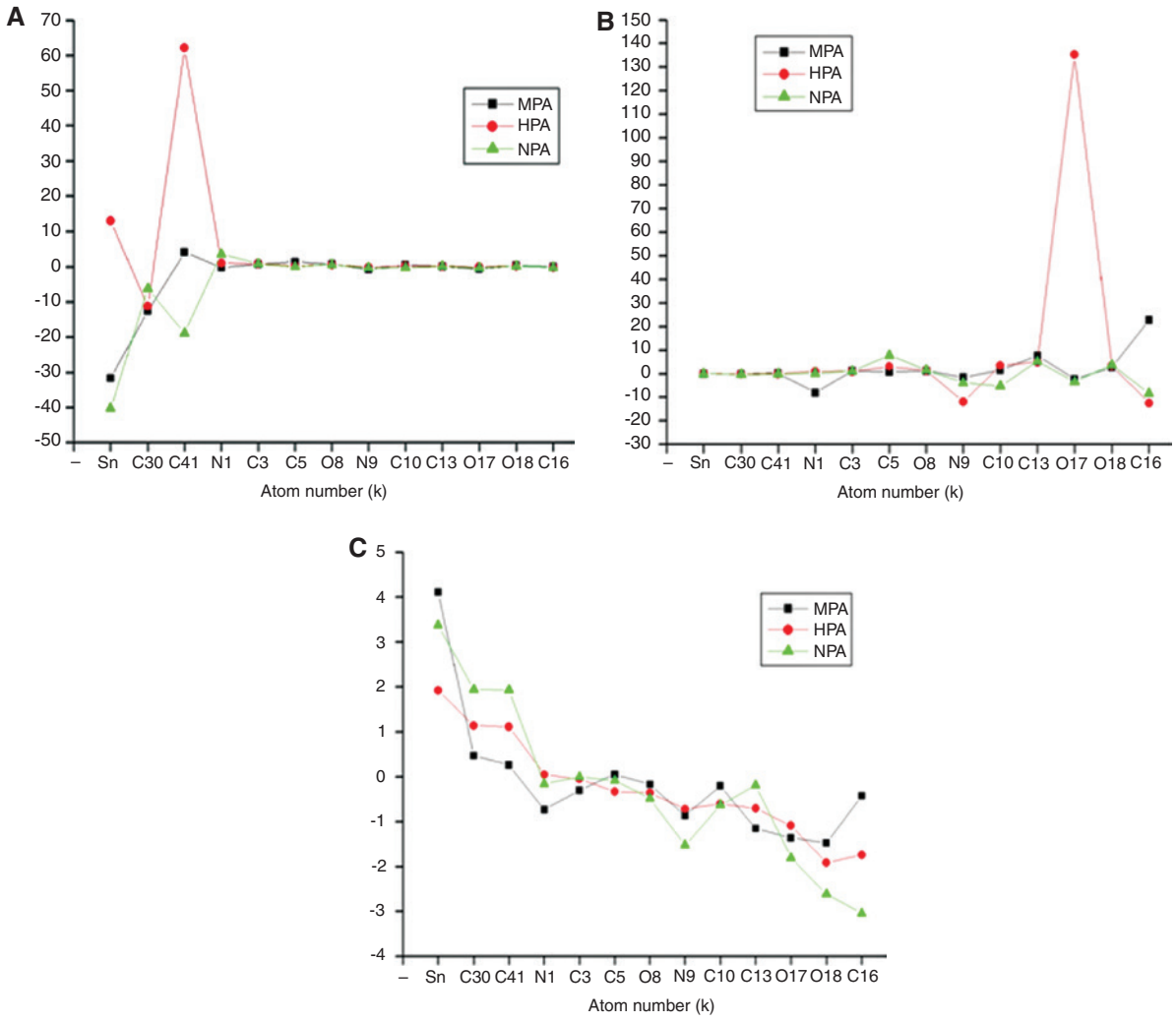

Figure 5: Variation of (A) relative electrophilicity, (B) relative nucleophilicity, and (C) dual reactivity descriptor at the selected atoms of Ph_2SnL based on MPA, HPA, and NPA charges, calculated at the B3LYP/6-31G(d,p)/LANL2DZ(Sn) level of theory (all values in panel C are in eV).

coordination sphere around the central Sn atom, the positive value of $f^2(k)$ at the central Sn atom, the carbon atoms in the organic residues (covalently bonded to the central Sn atom), and $N1_{(amino)}$ indicates that these sites are favored for the nucleophilic attack, whereas the negative value of $f^2(k)$ at $N9_{(peptidic)}$ and $O17_{(carboxylate)}$ indicates that these sites are favored for an electrophilic attack.

Conclusion

The present study significantly demonstrates the efficacy of quantum-chemical methods in studying the electronic structure of diphenyltin(IV) derivative of glycylphenylalanine at the B3LYP/6-31G(d,p)/LANL2DZ(Sn) level of theory, which will have greater ramifications in getting the vital insight into the structural features of the complex as also to gain insight into the plausible mechanism for their reactivity, specifically upon interaction with macromolecular receptors. The calculated values for the coordinating bond length and various other geometrical parameters in Ph_2SnL are closer to those reported for other organotin(IV) complexes with heterodonor atoms.

The conceptual DFT-based global and local reactivity descriptors have been effectively calculated on the basis of MPA, HPA, and NPA schemes. The calculated global reactivity descriptors indicate that complexation leads to softness in Ph_2SnL relative to H_2L. There seem to be some discrepancies in the calculation of conceptual DFT-based local reactivity descriptors on the basis of MPA and NPA schemes. However, irrespective of the population scheme, these descriptors can convincingly explain the charge distribution at all the atoms of Ph_2SnL and noticeably identify various nucleophilic and electrophilic sites within the

complex, which will further provide some mechanistic insight into the structure and reactivity of organotin(IV) complexes with heterodonor atoms, apart from its biological activity.

The theoretical calculations performed have identified the FMOs for Ph_2SnL, wherein the HOMO is concentrated over the dipeptide unit and the LUMO is concentrated around the central Sn atom encompassing phenyl moiety bonded to the central Sn atom.

Experimental

Computational details

All the quantum-chemical calculations have been performed using the Gaussian 09 program package (Frisch et al., 2010). The molecular geometries of glycylphenylalanine (H_2L) and Ph_2SnL were fully optimized in the gas phase at the DFT level using the B3LYP functional, which is a combination of Becke's three parameter (B3) gradient corrected hybrid exchange functional (Becke, 1993), with the dynamical correlation functional of Lee et al. (1988) (LYP). All the atoms except Sn were described by the 6-31G(d,p) basis set, which contains a reasonable number of basis set functions that are able to reproduce the experimental observations. The Sn atom in Ph_2SnL was described by the LANL2DZ basis set in which Sn inner shells are described by effective core potential ECP46MWB ($1s^22s^22p^63s^23p^63d^{10}4s^24p^64d^{10}$) along with the basis set (3s3p)/[2s2p] (Hay and Wadt, 1985). The geometry optimization was conducted through an algorithm of iterative steps to locate true global minima on the PES with default parameters for convergence is met. The absence of an imaginary frequency in a harmonic frequency calculation conducted at the same level of theory indicates that the calculated geometry is a true global minimum on the PES. The atomic charges at all the atoms in the studied systems were calculated using MPA, HPA, and NPA at the same level of theory. The energies of FMOs and the conceptual DFT-based global and local reactivity descriptors based on MPA, HPA, and NPA have been calculated for the studied systems using finite difference approximation (Geerlings et al., 2003). The MEP maps and the visualization of all results have been performed using Gauss View 5.0 (Dennington et al., 2009).

Acknowledgments: The authors are thankful to Banaras Hindu University, Varanasi, for providing basic infrastructural and computational facilities.

References

Alama, A.; Tasso, B.; Novelli, F.; Sparatore, F. Organometallic compounds in oncology: implications of novel organotins as antitumor agents. *Drug Discov. Today.* **2009**, *14*, 500–508.

Arjmand, F.; Parveen, S.; Tabassum, S.; Pettinari, C. Organo-tin antitumour compounds: their present status in drug development and future perspectives. *Inorg. Chim. Acta*. **2014**, *423*, 26–37.

Becke, A. D. Density functional thermochemistry. III. The role of exact exchange. *J. Chem. Phys*. **1993**, *98*, 5648–5652.

Carraher, C. E.; Roner, M. R. Organotin polymers as anticancer and antiviral agents. *J. Organomet. Chem.* **2014**, *751*, 67–82.

Chattaraj, P. K.; Sarkar, U.; Roy, D. R. Electrophilicity index. *Chem. Rev.* **2006**, *106*, 2065–2091.

Dennington II, R. D.; Keith, T. A.; Millam, J. M. Gauss View 5.0. Gaussian, Inc.: Wallingford CT, 2009.

Foresman, J. B.; Frisch, E. Exploring Chemistry with Electronic Structure Methods. Gaussian, Inc.: Pittsburgh, USA, 1996.

Frisch, M. J.; Trucks, G. W.; Schlegel, H. B.; Scuseria, G. E.; Robb, M. A.; Cheeseman, J. R.; Scalmani, G.; Barone, V.; Mennucci, B.; Petersson, G. A.; et al. Gaussian09, Revision B.01. Gaussian, Inc.: Wallingford, CT, 2010.

Geerlings, P.; De Proft, F.; Langenaeker, W. Conceptual density functional theory. *Chem. Rev.* **2003**, *103*, 1793–1873.

Girasolo, M. A.; Rubino, S.; Portanova, P.; Calvaruso, G.; Ruisi, G.; Stocco, G. New organotin(IV) complexes with L-arginine, N_α-*t*-Boc-L-arginine and L-alanyl-L-arginine: synthesis, structural investigations and cytotoxic activity. *J. Organomet. Chem.* **2010**, *695*, 609–618.

Girichev, G. V.; Giricheva, N. I.; Koifman, O. I.; Minenkov, Y. V.; Pogonin, A. E.; Semeikin, A. S.; Shlykov, S. A. Molecular structure and bonding in octamethyl-porphyrin tin(II), $SnN_4C_{28}H_{28}$. *Dalton Trans*. **2012**, *41*, 7550–7558.

Hay, P. J.; Wadt, W. R. Ab initio effective core potentials for molecular calculations-potentials for K to Au including the outermost core orbitals. *J. Chem. Phys.* **1985**, *82*, 299–310.

Huber, F.; Haupt, H. J.; Preut, H.; Barbieri, R.; LoGuidice, M. T. Preparation, crystal and molecular structure of diphenyltin-glycylglycinate $(C_6H_5)_2SnC_4H_6N_2O_3$. *Z. Anorg. Allg. Chem.* **1977**, *432*, 51–57.

Katsoulakou, E.; Tiliakos, M.; Papaefstathiou, G.; Terzis, A.; Raptopoulou, C.; Geromichalos, G.; Papazisis, K.; Papi, R.; Pantazaki, A.; Kyriakidis, D.; et al. Diorganotin(IV) complexes of dipeptides containing the α-aminoisobutyryl residue (Aib): preparation, structural characterization, antibacterial and antiproliferative activities of $[(n\text{-}Bu)_2Sn(H\text{-}_1L)]$ (LH = H-Aib-L-Leu-OH, H-Aib-L-Ala-OH). *J. Inorg. Biochem.* **2008**, *102*, 1397–1405.

Latrous, L.; Tortajada, J.; Haldys, V.; Léon, E.; Correia, C.; Salpin, J.-Y. Gas-phase interactions of organotin compounds with glycine. *J. Mass. Spectrom*. **2013**, *48*, 795–806.

Lee, C.; Yang, W.; Parr, R. G. Development of the Colle-Salvetti correlation-energy formula into a functional of the electron density. *Phys. Rev. B*. **1988**, *37*, 785–789.

Matczak, P. Theoretical investigation of the N→Sn coordination in $(Me_3SnCN)_2$. *Struct. Chem.* **2015**, *26*, 301–318.

Morell, C.; Grand, A.; Toro-Labbé, A. New dual descriptor for chemical reactivity. *J. Phys. Chem. A* **2005**, *109*, 205–212.

Mundus-Glowacki, B.; Huber, F.; Preut, H.; Ruisi, G.; Barbieri, R. Synthesis and spectroscopic characterization of dimethyl-, di-n-butyl, di-t-butyl- and diphenyl-tin(IV) derivatives of dipeptides: crystal and molecular structure of di-n-butyltin(IV) glycylvalinate. *Appl. Organometal. Chem*. **1992**, *6*, 83–94.

Nath, M. Toxicity and the cardiovascular activity of organotin compounds: a review. *Appl. Organometal. Chem.* **2008**, *22*, 598–612.

Nath, M.; Pokharia, S.; Eng, G.; Song, X.; Kumar, A. Diorganotin(IV) derivatives of dipeptides containing at least one essential amino acid residue: synthesis, characteristic spectral data,

cardiovascular, and anti-inflammatory activities. *Synth. React. Inorg. Met.-Org. Chem.* **2004**, *34*, 1689–1708.

Nath, M.; Singh, H.; Eng, G.; Song, X. New di- and triorganotin(IV) derivatives of tyrosinylphenylalanine as models for metal-protein interactions: synthesis and structural characterization. Crystal structure of Me_2Sn(Tyr-Phe).MeOH. *J. Organomet. Chem.* **2008**, *693*, 2541–2550.

Nath, M.; Singh, H.; Kumar, P.; Kumar, A.; Song, X.; Eng, G. Organotin(IV) tryptophanylglycinates: potential nonsteroidal anti-inflammatory agents; crystal structure of dibutyltin(IV) tryptophanylglycinate. *Appl. Organometal. Chem.* **2009**, *23*, 347–358.

Parr, R. G.; Pearson, R. G. Absolute hardness: companion parameter to absolute electronegativity. *J. Am. Chem. Soc.* **1983**, *105*, 7512–7516.

Parr, R. G.; Yang, W. Density functional approach to the frontier-electron theory of chemical reactivity. *J. Am. Chem. Soc.* **1984**, *106*, 4049–4050.

Parr, R. G.; Szentpály, L. V.; Liu, S. Electrophilicity index. *J. Am. Chem. Soc.* **1999**, *121*, 1922–1924.

Pellerito, L.; Nagy, L. Organotin(IV)$^{n+}$ complexes formed with biologically active ligands: equilibrium and structural studies, and some biological aspects. *Coord. Chem. Rev.* **2002**, *224*, 111–150.

Pokharia, S. Theoretical insights on organotin(IV)-protein interaction: density functional theory (DFT) studies on di-n-butyltin(IV) derivative of glycylvaline. *Asian J. Res. Chem.* **2015**, *8*, 7–12.

Politzer, P.; Laurence, P. R.; Jayasuriya, K. Molecular electrostatic potentials: an effective tool for the elucidation of biochemical phenomena. *Env. Health. Perspec.* **1985**, *61*, 191–202.

Reed, A. E.; Wienstock, R. B.; Weinhold, F. Natural population analysis. *J. Chem. Phys.* **1985**, *83*, 735–746.

Roy, R. K.; Krishnamurti, S.; Geerlings, P.; Pal, S. Local softness and hardness based reactivity descriptors for predicting intra- and intermolecular reactivity sequences: carbonyl compounds. *J. Phys. Chem. A* **1998**, *102*, 3746–3755.

Roy, R. K.; Saha, S. Studies of regioselectivity of large molecular systems using DFT based reactivity descriptors. *Annu. Rep. Prog. Chem., Sect. C* **2010**, *106*, 118–162.

Saha, S.; Bhattacharjee, R.; Roy, R. K. Hardness potential derivatives and their relation to Fukui indices. *J. Comput. Chem.* **2013**, *34*, 662–672.

Thomas, R.; Nelson, J. P.; Pardasani, R. T.; Pardasani, P.; Mukherjee, T. Novel tin complexes containing an oximato ligand: synthesis, characterization, and computational investigation. *Helv. Chim. Acta* **2013**, *96*, 1740–1749.

Yang, W.; Parr, R. G. Hardness, softness, and the fukui function in the electronic theory of metals and catalysis. *Proc. Natl. Acad. Sci. U.S.A.* **1985**, *82*, 6723–6726.

Supplemental Material: The online version of this article (DOI: 10.1515/mgmc-2016-0009) offers supplementary material, available to authorized users.